

Thermalization of magnetically trapped metastable helium

A. Browaeys, A. Robert, O. Sirjean, J. Poupard, S. Nowak, D. Boiron, C. I. Westbrook, and A. Aspect
Laboratoire Charles Fabry de l'Institut d'Optique, UMR 8501 du CNRS, Boite Postale 147, F-91403 Orsay Cedex, France

(Received 21 February 2001; published 10 August 2001)

We have observed thermalization by elastic collisions of magnetically trapped metastable helium atoms. Our method directly samples the reconstruction of a thermal energy distribution after the application of a RF knife. The relaxation time of our sample toward equilibrium gives an elastic collision rate constant of $\alpha \sim 5 \times 10^{-9} \text{ cm}^3/\text{s}$ at a temperature of 1 mK. This value is close to the unitarity limit.

DOI: 10.1103/PhysRevA.64.034703

PACS number(s): 34.50.-s, 32.80.Pj, 51.10.+y, 67.65.+z

Bose-Einstein condensation (BEC) of dilute atomic vapors has been observed in Rb [1], Na [2], Li [3], and H [4]. Atoms in these gases are in their electronic ground states. Metastable helium in the 2^3S_1 state (He^*), which has long been of interest to the laser cooling community, is by contrast in a state 20 eV above the ground state. This situation presents additional possibilities for the study of cold dilute atomic gases. First, the large internal energy permits efficient detection by ionization of other atoms and surfaces: it is possible to study very small samples. Second, Penning ionization both by the background gas and between trapped atoms offers a high time resolution monitor of the number and density of trapped atoms. Third, the possibility of using the large internal energy of He^* for atomic lithography has already been demonstrated [5], and this application as well as atom holography [6] may benefit from highly coherent sources. Finally, much theoretical work has already been devoted to estimation of the elastic collision cross sections on the one hand and Penning ionizing rates on the other [7,8]. Experiments such as the one reported here can test this work.

BEC is achieved in dilute gases by evaporative cooling of a magnetically trapped sample [9]. In He^* , it is hampered by the fact that in a magneto-optical trap, the typical starting point of magnetic trapping, the achievable atomic density is limited by a large light-assisted Penning ionization rate [10–15]. On the other hand, the scattering length for low energy elastic collisions is predicted to be quite large, and the Penning ionization rate highly suppressed in a spin polarized sample [7,8]. He^* in a magnetic trap necessarily constitutes a spin polarized sample and experiments have already demonstrated a suppression of more than one order of magnitude [16–18]. If the theoretical estimates are right, efficient evaporative cooling may still be possible in spite of the low initial trap density. We report here the observation of the thermalization of He^* due to elastic collisions which appears to roughly bear out the predictions.

To perform a thermalization experiment, a trapped cloud is deliberately placed out of equilibrium and its relaxation due to the elastic collisions between trapped particles is observed. Usually the observations are made by imaging the spatial distribution as a function of time [19–21]. In our experiment the relaxation is observed directly in the energy distribution of the atoms in the magnetic trap. First this distribution is truncated above $E_{\text{RF}} = h\nu$ by a radio frequency pulse (or RF knife) of frequency ν . The cloud rethermalizes by elastic collisions and the population of the states of en-

ergy higher than E_{RF} increases from zero; for large times compared to the thermalization time τ_{th} the distribution reaches a thermal distribution [22]. With the help of an analytical model and numerical simulations, we deduce τ_{th} from the time dependence of the number of atoms with energy above E_{RF} . We measure this time dependence by applying a second RF knife after a delay time t , and with a frequency slightly above that of the first one. Our model also allows us to relate τ_{th} to the elastic collision rate per atom in the trap.

Much of our setup has been described previously [14,17]. Briefly, we use a liquid N_2 cooled dc discharge source to produce a beam of metastable He atoms. The beam is slowed down to ~ 100 m/s using Zeeman slowing and loads a magneto-optical trap (MOT). Typically, 3×10^8 atoms are trapped at a peak density of $3 \times 10^9 \text{ at./cm}^3$, limited by light-induced Penning ionization. The temperature of the cloud is about 1 mK and the cloud is roughly spherical with a rms size of 2.5 mm. We then apply a 5 ms Doppler molasses to cool the atoms down to 300 μK . This is achieved by switching off the magnetic field, decreasing the detuning close to resonance, and lowering the intensity to 10% of its value in the MOT. An optical pumping step allows us to trap up to 1.5×10^8 atoms in a Ioffe-Pritchard trap. We use a “cloverleaf” configuration [23] with $B' = 85 \text{ G/cm}$, $B'' = 25 \text{ G/cm}^2$, and a bias field $B_0 = 200 \text{ G}$. The two sets of coils are outside the vacuum, separated by 4 cm. After lowering the bias field to 4 G, the temperature of the compressed atomic sample reaches 1 mK. The lifetime of the trap is 60 s.

We use a two stage microchannel plate (MCP) to detect the atoms. The MCP is placed 5 cm below the trapping region and has an active area of 1.4 cm diameter. Two grids above the MCP allow us to repel all charged particles and detect only the He^* . After turning off the magnetic trap, the MCP signal corresponds to a time of flight (TOF) spectrum that gives the temperature of the atoms. The area of this spectrum is proportional to the number of atoms in the trap at the time it was turned off. The collection and detection efficiency of the MCP varies by roughly a factor of 2 depending on the magnetic field configuration we use, and so one must take care to use only data corresponding to the same magnetic field when making comparisons. We also use the MCP to monitor the atoms falling out of the trap while applying a RF knife. The area of the MCP signal in this case measures the number of atoms with an energy above that of the RF knife. Finally, when we bias the grids so as to attract positive

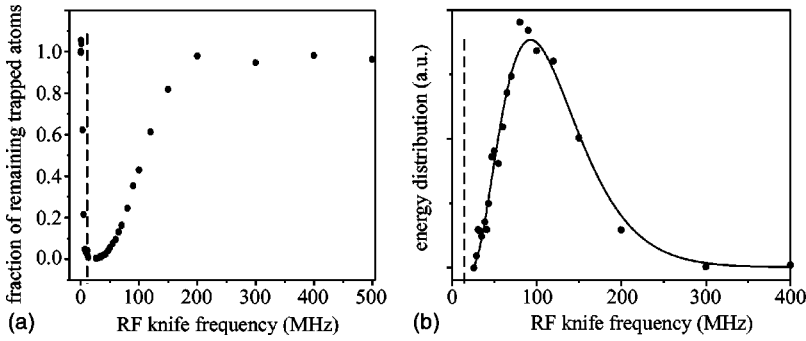


FIG. 1. RF spectrum of atoms in the magnetic trap. (a) Fraction of remaining trapped atoms after the RF pulse as a function of the RF frequency ν . (b) Derivative of these data, i.e., the energy distribution in the magnetic trap. The solid line is the prediction for a cloud at a temperature of 1.1 mK, the temperature measured by time of flight (TOF). The dashed line indicates the frequency corresponding to the bias field.

ions, the MCP signal can be used to observe the products of Penning ionization with the background gas while the trap is on. This signal is proportional to the number of trapped atoms. We observe an exponential decay, indicating that two body loss ($\text{He}^* + \text{He}^*$) is negligible.

Two parallel coils in the vacuum system produce a RF magnetic field perpendicular to the bias field and constitute the RF knife. To understand the effect of the RF knife on the trapped cloud and to assure that our sample is at thermal equilibrium, we first performed a RF spectroscopy measurement of the energy of the atoms in the trap [24]. We apply a RF pulse at a frequency $h\nu$ which changes the Zeeman sub-level of the atoms from the trapped $M = +1$ state to $M = 0$. The duration of the knife is 3 s, which is necessary to expel all the atoms with energy above $h\nu$ over the entire range that we explore. We then turn off the magnetic trap to measure the number of remaining atoms. Observation of the atoms falling onto the MCP during the RF knife shows that the flux of atoms expelled is negligible at the end of the pulse.

An example of the RF spectrum is shown in Fig. 1(a). The derivative of the data gives the energy distribution. In Fig. 1(b) we compare this distribution with a thermal one at 1.1 mK, the temperature measured by an independent TOF measurement. We conclude that our atomic sample is close to thermal equilibrium.

We begin the thermalization experiment with a 2 s RF knife of frequency $\nu_1 = 135$ MHz [corresponding to $\eta = (h\nu - 2\mu_B B_0)/k_B T \sim 6$]. Next we measure the number of atoms falling onto the MCP during a second RF knife at a slightly higher frequency ($\nu_2 = 138$ MHz) and delayed by a time t . Assuming that the angular distribution of the atoms expelled by the second RF knife is constant during the thermalization process, the MCP signal is proportional to the number of expelled atoms. Furthermore, we have checked that the difference of the TOF areas before and after application of the RF knife agrees to within 20% with the number of atoms that should be expelled by the knife, given our temperature and the position of the knife. This gives us confidence that at the end of the RF knife the energy distribution is a truncated Maxwell-Boltzmann distribution, and that the sufficient ergodicity hypothesis we make below is reasonable.

Plots of the number of expelled atoms as a function of t are shown in Fig. 2 for samples having different numbers of atoms but the same temperature to within 10%. Figure 2 shows that the number of atoms above the RF knife increases rapidly and then falls again with a time constant close to the

trap lifetime as atoms are lost. If the initial increase is indeed due to thermalizing collisions, the initial slope of each curve should be proportional to the square of the number of atoms. Our data roughly confirm this dependence.

To be more quantitative, and to determine the thermalization time τ_{th} , we use a model based on the Boltzmann equation under the sufficient ergodicity hypothesis and inspired by [25]. We divide the sample into two energy regions \mathcal{E}_- and \mathcal{E}_+ with energies below and above $\eta k_B T$, respectively, and denote by N_- and N_+ the number of atoms belonging to the two regions. We assume that $\eta \gg 1$. Immediately after truncation, $N_+ = 0$, and we seek a differential equation governing the time dependence of N_+ . Since $\eta \gg 1$, we take into account only collisions of the type $(\mathcal{E}_-) + (\mathcal{E}_-) \leftrightarrow (\mathcal{E}_-) + (\mathcal{E}_+)$, and neglect all collisions involving two atoms in \mathcal{E}_+ in either the final or initial state. The corresponding flux \dot{N}_+ is thus of the form

$$\dot{N}_+ = \Delta_1 N_-^2 - \Delta_2 N_- N_+. \quad (1)$$

The coefficients Δ_1 and Δ_2 are calculated using Boltzmann equation [27]. In particular, $\Delta_1 N_-$ is exactly the evaporation rate in an evaporative cooling process [25]. If we make the further approximations that the atoms in \mathcal{E}_- and \mathcal{E}_+ have thermal distributions [26], neglect variations of the temperature during thermalization, and assume that the collision cross section σ is independent of velocity, Δ_1 and Δ_2 are analytic functions of the trap parameters, atomic mass m , σ ,

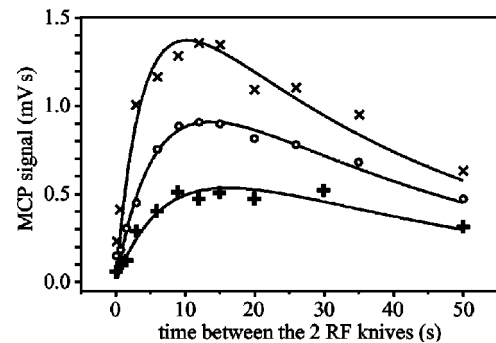


FIG. 2. Integrated MCP signal during the RF probe pulse as a function of the delay between the truncation and probe pulses. The three curves correspond to 5×10^7 , 7×10^7 , and 10×10^7 atoms in the trap, varied by changing the power in the Zeeman slowing laser. The lifetime of the trap is 38 ± 4 s, and the temperature is 0.9 ± 0.1 mK.

η , and $\mu_B B_0/k_B T$. This last parameter appears because our trap cannot be approximated by a harmonic trap; we use the semilinear form [25]. It is straightforward to take into account the finite lifetime τ of the atomic sample since $N_-(t) + N_+(t) = N_-(0)\exp(-t/\tau)$. The solution of the resulting differential equation is

$$N_+(t) = N_{\text{th}} e^{-t/\tau} \left[1 + \frac{q}{1 - q - \exp[(\tau/\tau_{\text{th}})(1 - e^{-t/\tau})]} \right], \quad (2)$$

where $\tau_{\text{th}}^{-1} = (\gamma_{\text{el}}/\sqrt{2})[q/(1-q)](e^{-\eta} V_{\text{ev}}/V_e)$ and $N_{\text{th}} = (1-q)N_-(0)$. The elastic collision rate is $\gamma_{\text{el}} = n\sigma\bar{v}$ with n defined at the center of the trap and $\bar{v} = 4\sqrt{k_B T/\pi m}$. The quantities V_{ev} , V_e , and q are defined as in [25,27]; they are analytic functions of η and $\mu_B B_0/k_B T$. The quantity q is the ratio of the number of atoms below the RF knife to the total for a thermal distribution (about 0.9 under our conditions), and N_{th} is the asymptotic value of N_+ for infinite trap lifetime. Numerical simulations of the energy form of the Boltzmann equation are in good agreement with our model for $\eta > 10$; for $\eta = 6$ the quantity $\gamma_{\text{el}}\tau_{\text{th}}$ is 1.8 times larger, meaning that our assumption about the distribution function fails for small η [27]. We take this factor into account in calculating γ_{el} .

To fit the data of Fig. 2 with Eq. (2), we fix the lifetime τ at its measured value and use τ_{th} and N_{th} as adjustable parameters. The uncertainty in τ_{th} is estimated by varying the lifetime of the trap within its uncertainty range and looking at the resulting dispersion in τ_{th} . The uncertainty in the number of trapped atoms is estimated from the dispersion of the TOF area measurements before and after taking a curve as in Fig. 2. The exact value of q has little influence on the fit.

We made several tests to check the consistency of our results. First, we checked that the fitted value of N_{th} corresponds to the expected fraction of atoms above the knife for our temperature. Second, Fig. 3 shows that τ_{th}^{-1} is proportional to the number of trapped atoms, as it must be if the process of refilling of the upper energy class is due to two body collisions. We can exclude any effect independent of the number of atoms. The line passing through the origin uses the slope as a fit parameter and has $\chi^2 = 5$ for eight degrees of freedom. Third, we have done an additional experiment that confirms the presence of elastic collisions: in a trap decay rate experiment, *in the presence* of the RF knife, the ion signal exhibits a clear nonexponential behavior at short times. This effect can be satisfactorily interpreted as elastic collisions bringing atoms above the RF knife and hence allows a measurement of the evaporation rate. This

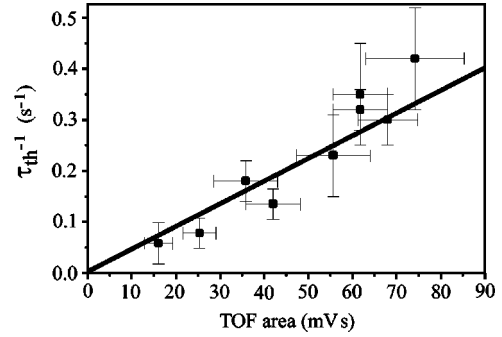


FIG. 3. Thermalization rate τ_{th}^{-1} versus the area of the corresponding TOF spectrum (proportional to the number of trapped atoms). The solid line shows a linear fit constrained to pass through the origin.

rate is consistent with the results obtained in our thermalization experiment. Fourth, we have checked that heating cannot explain the repopulation of the upper energy classes. With the trap undisturbed, we can place an upper limit on the heating rate of $25 \mu\text{K}$ in 60 s. This limit is two orders of magnitude too low to explain our data. Lastly, we have performed the thermalization experiment for different lifetimes of the magnetic trap (20, 40, and 60 s) and found consistent results.

From our data in Fig. 3, we can deduce an accurate measurement of the thermalization time; the fit gives $\tau_{\text{th}} = 3.0 \pm 0.3$ s for the densest sample. Using the measured temperature and bias field, this value of τ_{th} leads to $\gamma_{\text{el}} = 6 \pm 1$ s $^{-1}$; this result depends on the accuracy of our thermalization model. To find the rate constant $\alpha = \gamma_{\text{el}}/n$, we must estimate the density. Since the data show that our sample is close to thermal equilibrium, we can calculate the volume of the trap knowing the trap parameters. The absolute measurement of the number of atoms is performed by measuring the total power absorbed from a saturating laser beam, similar to [15]. A TOF area of 75 mV s corresponds to 10^8 atoms in the magnetic trap with an uncertainty of a factor of 2. This leads to $\alpha = 5 \times 10^{-9}$ cm 3 /s to within a factor of 3 at $T = 1 \pm 0.1$ mK. Leduc *et al.* have obtained a similar result with a different measurement [28]. The unitarity limit at that temperature is $\alpha \sim 10^{-8}$ cm 3 /s. This means that it is probably not valid to use a constant elastic cross section in our model and some deviation might appear in the quantity $\gamma_{\text{el}}\tau_{\text{th}}$. The results shown here are very encouraging for evaporative cooling of He* in search of BEC.

We thank P. Leo and P. Julienne and the ENS helium group for helpful discussions. This work was partially supported by the EC under Contract No. IST-1999-11055 and No. HPRN-CT-2000-00125, and DGA Grant No. 99.34.050.

- [1] C.J. Anderson, J.R. Ensher, M.R. Matthews, C.E. Wieman, and E.A. Cornell, *Science* **269**, 198 (1995).
 [2] K.B. Davis, M.O. Mewes, M.R. Andrews, N.J. van Druten, D.S. Durfee, D.M. Kurn, and W. Ketterle, *Phys. Rev. Lett.* **75**, 3969 (1995).

- [3] C.C. Bradley, C.A. Sackett, J.J. Tollett, and R.G. Hulet, *Phys. Rev. Lett.* **75**, 1687 (1995).
 [4] D.G. Fried, T.C. Killian, L. Willmann, D. Landhuis, S.C. Moss, D. Kleppner, and T.J. Greytak, *Phys. Rev. Lett.* **81**, 3811 (1998).

- [5] S. Nowak, T. Pfau, and J. Mlynek, *Appl. Phys. B: Lasers Opt.* **63**, 203 (1996); A. Bard *et al.*, *J. Vac. Sci. Technol. B* **15**, 1805 (1997).
- [6] J. Fujita, M. Morinaga, T. Kishimoto, M. Yasuda, S. Matsui, and F. Shimizu, *Nature (London)* **380**, 691 (1996).
- [7] G. Shlyapnikov, J. Walraven, U. Rahmanov, and M. Reynolds, *Phys. Rev. Lett.* **73**, 3247 (1994); P. Fedichev, M. Reynolds, U. Rahmanov, and G. Shlyapnikov, *Phys. Rev. A* **53**, 1447 (1996).
- [8] V. Venturi, I.B. Whittingham, P.J. Leo, and G. Peach, *Phys. Rev. A* **60**, 4635 (1999); V. Venturi, I.B. Whittingham, and J.F. Babb, e-print physics/0011072.
- [9] H.F. Hess, *Phys. Rev. B* **34**, 3476 (1986).
- [10] F. Bardou, O. Emile, J.M. Courty, C.I. Westbrook, and A. Aspect, *Europhys. Lett.* **20**, 681 (1992).
- [11] H.C. Mastwijk, J.W. Thomsen, P. van der Straten, and A. Niehaus, *Phys. Rev. Lett.* **80**, 5516 (1998).
- [12] P.J.J. Tol, N. Herschbach, E.A. Hessels, W. Hogervorst, and W. Vassen, *Phys. Rev. A* **60**, 761 (1999).
- [13] M. Kumakura and N. Morita, *Phys. Rev. Lett.* **82**, 2848 (1999).
- [14] A. Browaeys *et al.*, *Eur. Phys. J. D* **8**, 199 (2000).
- [15] F. Pereira Dos Santos, F. Perales, J. Léonard, A. Sinatra, Junmin Wang, F.S. Pavone, E. Rasel, C.S. Unnikrishnan, and M. Leduc, *Eur. Phys. J. D* **14**, 15 (2001).
- [16] J.C. Hill, L.L. Hatfield, N.D. Stockwell, and G.K. Walters, *Phys. Rev. A* **5**, 189 (1972).
- [17] S. Nowak, A. Browaeys, J. Poupard, A. Robert, D. Boiron, C.I. Westbrook, and A. Aspect, *Appl. Phys. B: Lasers Opt.* **70**, 455 (2000).
- [18] N. Herschbach, P.J.J. Tol, W. Hogervorst, and W. Vassen, *Phys. Rev. A* **61**, 050702(R) (2000).
- [19] C.R. Monroe, E.A. Cornell, C.A. Sackett, C.J. Myatt, and C.E. Wieman, *Phys. Rev. Lett.* **70**, 414 (1993).
- [20] K.B. Davis, M.O. Mewes, M.A. Joffe, M.R. Andrews, and W. Ketterle, *Phys. Rev. Lett.* **74**, 5202 (1995).
- [21] M. Arndt, M. Ben Dahan, D. Guéry-Odelin, M.W. Reynolds, and J. Dalibard, *Phys. Rev. Lett.* **79**, 625 (1997).
- [22] D.W. Snoke and J.P. Wolfe, *Phys. Rev. B* **39**, 4030 (1989).
- [23] M.O. Mewes, M.R. Andrews, N.J. van Druten, D.M. Kurn, D.S. Durfee, and W. Ketterle, *Phys. Rev. Lett.* **77**, 416 (1996).
- [24] A.G. Martin, K. Helmerson, V.S. Bagnato, G.P. Lafyatis, and D.E. Pritchard, *Phys. Rev. Lett.* **61**, 2431 (1988).
- [25] O.J. Luiten, M.W. Reynolds, and J.T.M. Walraven, *Phys. Rev. Lett.* **53**, 382 (1996).
- [26] This hypothesis is legitimate in \mathcal{E}_- because it is true at $t=0$ and because only few particles will leave this region; one can find indications in [22] that this hypothesis is not too strong in \mathcal{E}_+ .
- [27] D. Boiron *et al.* (unpublished).
- [28] M. Leduc (private communication).